Braking Capabilities on Flooded Runways: Flight Test Results Obtained with a Business Jet

Gerard W.H. van Es[1]
NLR - Netherlands Aerospace Centre, P.O. Box 90502, 1006 BM Amsterdam, The Netherlands

Statistics show that the likelihood of a runway excursion during takeoff or landing is much higher on flooded runways than on dry runways. Extreme loss of tyre braking can occur during rejected takeoffs and landings on flooded runways. As a result the stopping distance increases significantly and could exceed the available runway length. Most research in the past has focused on the braking capabilities of aircraft on wet runways instead of flooded runways. Most of the knowledge of aircraft braking performance on flooded runways was gained with older aircraft designs. This knowledge is still used to determine the takeoff and landing performance of today's modern aircraft. During the development of the European Action Plan for the Prevention of Runway Excursions it was recognised that current aircraft designs may act differently when braking on water flooded runways from aircraft tested earlier, due to new tyres and anti-skid system designs. Also the water depths during these earlier tests were often just above the wet-flooded runway threshold. Flight tests with more modern aircraft designs were therefore scheduled as part of a research project under EU's Horizon 2020 Research and Innovation Programme. This paper summarises the flight tests conducted with a Cessna Citation II aircraft on a flooded runway. Unbraked and braked tests were conducted in a specially constructed water pond at different ground speeds. Numerous parameters were recorded during each test run including accelerations, speeds, engine performance, etc. From the test data, effective braking friction for different grounds speeds were derived, contamination drag levels were established, and insight into the hydroplaning characteristics under unbraked and braked conditions were obtained.

Nomenclature

b_s	=	effective tyre width at water depth level
C_{Ds}	=	water displacement drag coefficient
d	=	water depth
f_H	=	hydroplaning decay correction
F_{brake_main}	=	braking force on the main gear tyres
N_{main}	=	normal load on the main gear tyres
S	=	reference area
V_g	=	ground speed
V_p	=	hydroplaning speed
W	=	tyre width (unloaded)
δ	=	tyre vertical deflection
ρ	=	density of water

I. Introduction

There are at least two runway excursions each week worldwide in which aircraft run off the side or end of a runway. Runway excursions are a persistent problem and their numbers have not decreased in more than 20 years. These facts bring attention to the need to identify measures to prevent runway excursions. The European

[1] Senior Consultant Aircraft Operations & Safety, NLR- Netherlands Aerospace Centre, vanes@nlr.nl.

Action Plan *Prevention of Runway Excursions* provides recommendations to reduce runway excursions. This Action Plan also identified areas were research is needed to further reduce runway excursion risk. The present paper discusses the results of one of the research topics addressed in the action plan, namely, *research on the impact of fluid contaminants of varying depth on aircraft stopping performance*. The fast majority of aircraft takeoffs and landings are conducted on dry runways. Only a small portion is conducted on non-dry runways like water contaminated (flooded) runways. Statistics show that the likelihood of a runway excursion during takeoff or landing is much higher on flooded runways than on dry runways. Extreme loss of tyre braking can occur during rejected takeoffs and landings on flooded runways. As a result the stopping distance increases significantly which could exceed the available runway length. Most research in the past has focused on the braking capabilities of aircraft on wet runways instead of flooded runways. Most of the knowledge of aircraft braking performance on flooded runways was gained during the late 60s, mid-70s, and late 80s using aircraft like the CV880, CV990, C141, C123B, B727-100, and the B737-100. The anti-skid systems and tyres installed on these aircraft are not representative for current aircraft designs. A number of the earlier tests were also conducted on runways flooded to an average water depth just above the wet-flooded runway threshold (3 mm depth). The knowledge gained on the braking performance with these older aircraft designs on flooded runways is still used to determine the takeoff and landing performance of today's modern aircraft. During the development of the *European Action Plan for the Prevention of Runway Excursions* it was recognised that current aircraft designs may act differently when braking on water contaminated runways. This paper presents the results of flight tests conducted on a specially prepared runway using a Cessna Citation business Jet operated by the National Aerospace Centre NLR. These flight tests were conducted as part of the Future Sky Safety project funded under EU's Horizon 2020 Research and Innovation Programme. Future Sky Safety is a Joint Research Programme (JRP) on Safety, initiated by EREA, the association of European Research Establishments in Aeronautics.

The main objective of the flight tests discussed in this paper is to collect data on braking friction coefficients with an aircraft having a fully modulating anti-skid system on a well flooded runway. These data can be used to validate models for predicting braking capabilities of modern aircraft on flooded runways.

Before discussing the test results obtained with the Cessna Citation Business Jet, a general introduction into braking on flooded runways is presented. The factors that influence aircraft tyre braking performance on flooded runways are discussed. The second part discusses anti-skid systems used on aircraft and their performance on flooded runways. The last part of technical paper presents the results obtained with a Cessna Business Jet Aircraft tested on a flooded runway. The paper also discusses in the preparations made including the construction of the test runway, flight test preparations, and the test procedures.

II. General introduction to braking on flooded runways

Extreme loss of tyre braking can occur during rejected takeoffs and landings of aircraft on flooded runways. The term hydroplaning, or aquaplaning, is used to describe this loss in traction on flooded runways. Hydroplaning is defined as the condition under which the tyre footprint is lifted off the runway surface by the action of the fluid. The forces from the fluid pressures balance the vertical loading on the wheel. Since fluids cannot develop shear forces of a magnitude comparable with the forces developed during dry tyre-runway contact, tyre traction under this condition drops to values significantly lower than on a dry runway. Water pressures developed on the surface of the tyre footprint and on the ground surface beneath the footprint originate from the effects of either fluid density and/or fluid viscosity, depending upon conditions. This has resulted in the classification of hydroplaning into two types, namely *dynamic* and *viscous hydroplaning*. Both types of hydroplaning can exist simultaneously and have the same impact on braking friction of the tyre. However, the factors influencing both types are different. To better understand the influence of both types of hydroplaning conditions, the contact surface of the tyre and the ground is divided into three zones[1]. Figure 1 illustrates the three zones under a tyre footprint of a braked or a free rolling tyre moving on a wet or flooded surface. In zone 1 the tyre contacts the stationary water film on the runway. The bulk volume of the water is being displaced in this zone. Zone 2 is a transition zone that consists of a thin water film. Finally zone 3 is a dry zone with no water film present between the tyre and the surface.

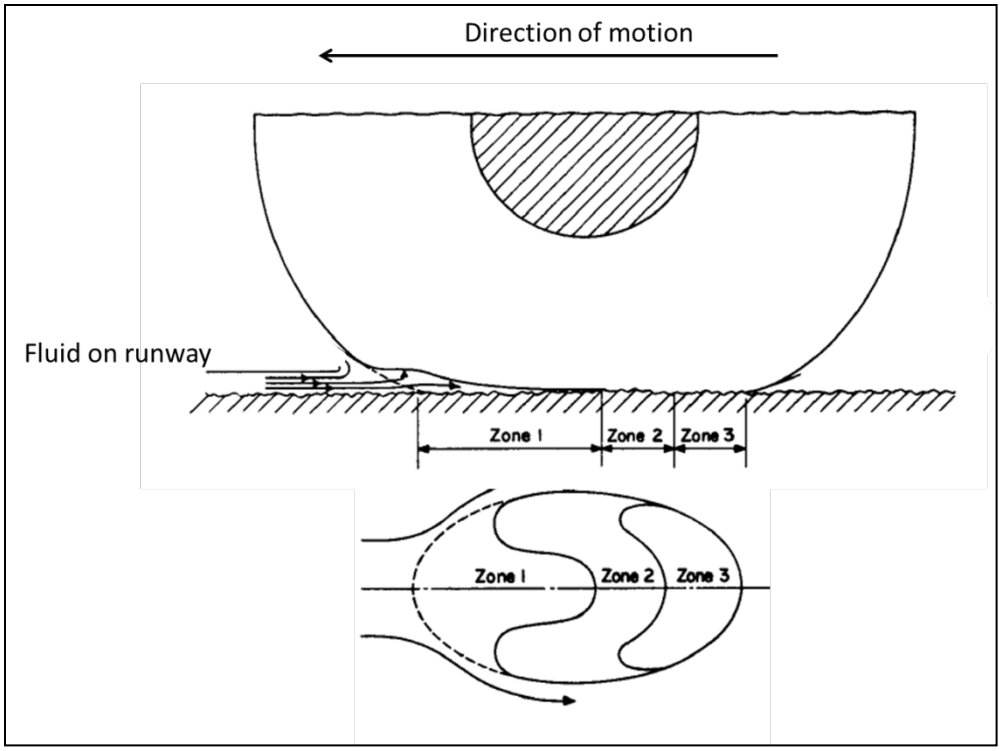

Figure 1: Zones under a tyre footprint when rolling along a wet/flooded surface[1].

In zone 1 much of the water is ejected as spray and squeezed through the tyre's tread and the runway texture. Hydroplaning in zone 1 is the result of the hydrodynamic forces developed when a tyre rolls on a water covered surface. This is a direct consequence of the tyre impact with the water which overcomes the fluid inertia. With increasing ground speed zone 1 extends further to the rear into the contact area. At a certain (high) ground speed, zone 1 can extend throughout the contact area. Zone 2 & 3 then no longer exist and the tyre becomes completely detached from the ground. This is called full dynamic hydroplaning. The critical ground speed at which this condition occurs is often called dynamic hydroplaning speed. When the condition of full dynamic hydroplaning is reached, the wheel speed drops. Dynamic hydroplaning is influenced by a number of factors like tyre inflation pressure, tyre tread, water depth and runway macrotexture. Macrotexture is the runway roughness formed by the large stones and/or grooves in the surface of the runway and provides escape channels to drain bulk water from zone 1. Macrotexture delays the build-up of fluid dynamic pressure to much higher speeds than the speeds found for pavements with no or little macrotexture. The tyre tread grooves in the tyre footprint are vented to atmosphere and provide escape channels for the bulk water trapped in zone 1. The tyre tread grooves act similar to the pavement macrotexture in draining the bulk water. When there is sufficient macrotexture on the surface and/or the tyre has a sufficient number of deep circumferential grooves, complete dynamic hydroplaning will normally not occur, unless the water depth is high enough so that both tyre grooves and runway macrotexture cannot drain the water sufficiently quick enough. Studies by NASA[2] in the 60s showed that on a well flooded runway aircraft tyres typically start to experience a full dynamic hydroplane condition when the forward speed (in knots) equals nine times the square root of the tyre inflation pressure (in psi). However later studies showed that this empirical equation does not apply to more recent tyre designs. This is illustrated in Figure 2, which shows experimental dynamic hydroplaning speeds obtained from full-scale tests for different aircraft tyre types under wide range of conditions (e.g. macrotexture depths, normal loads, water depths, and tyre groove depths). Basically all modern tyres shown in this figure have dynamic hydroplane speeds (well) below $9\sqrt{p}$. This is explained by the difference found in the tyre footprint aspect ratio which is the tyre footprint length over the footprint width[3]. From static load tests it follows that the tyre footprint aspect ratio of modern tyres is lower than for older designs of bias ply tyres of the same size and under equal conditions (inflation pressure and vertical load). As a result modern aircraft tyres tend to hydroplane at lower speeds that previously found for older tyre designs[3].

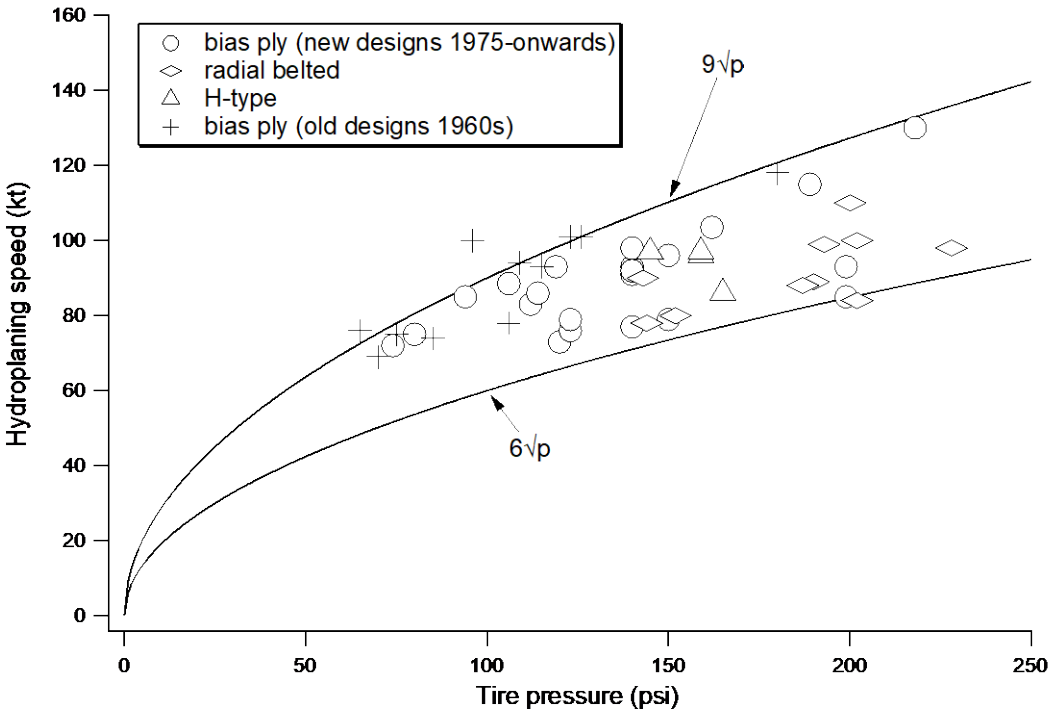

Figure 2: Dynamic hydroplaning speeds for different aircraft tyres as function of inflation pressure (mainly obtained from unpublished full scale aircraft tests[1]).

As shown in Figure 2, the classic NASA formula for predicting the full dynamic hydroplaning speed under spin-down conditions[2], 9√p, over-predicts the hydroplaning speed for modern aircraft tyres. This was already anticipated by some aircraft manufacturers which used a modified version of the classical dynamic hydroplaning equation for performance calculations during the late 70s. Following the simple NASA relation the available full scale experimental data suggest that a modern bias ply tyre would hydroplane (dynamically) on a well flooded runway at around 8.5√p, a H-type tyre at around 7.5√p and a radial tyre at around 6.9√p, with the speed in knots and p in psi[1]. These relations can be used for a first estimation of the spin-down dynamic hydroplaning speed in absence of experimental data.

Zone 2 is a transition region. There is only a thin film of water in this zone and water pressure is maintained by viscous effects (hence the name viscous hydroplaning). Viscous hydroplaning typically occurs on wet/flooded runways that have a smooth microtexture. Microtexture is the sandpaper like roughness of a surface formed by the sharpness of the fine grain particles on the individual stone particles of the surface. Pavement microtexture performs its function by providing the surface a large number of sharp pointed projections that, when contacted by the tyre tread, generate very high local bearing pressures. This intense pressure quickly breaks down the thin water film and allows the tyre to regain dry contact with the pavement surface texture[1]. Viscous hydroplaning can occur at ground speeds much lower than the speed for complete dynamic hydroplaning. Also the minimum water depth needed for viscous hydroplaning is much less than for dynamic hydroplaning. The pressure build-up in zone 2 is also much less dependent on ground speed compared to the pressure build-up in zone 1. For runways with a harsh microtexture, viscous hydroplaning is unlikely to occur as the microtexture penetrates and diffuses the thin water film. The area of zone 2 is relatively small or completely absent in this case. Circumferential grooves have a very small effect on removing the thin water film in zone 2.

Zone 3 is a region of dry contact. The friction forces on the tyre are generated in this zone when the wheel is braked. The friction force is approximately equal to the dry runway friction force times the ratio of the contact area in zone 3 and the overall tyre-ground contract area. Therefore the smaller zone 3 gets, the lower the braking friction forces become. When a tyre is fully separated by a film of water the braking friction coefficient for an aircraft tyre is very low as fluids cannot develop shear forces of a significant magnitude.

III. Aircraft anti-skid systems and flooded runways

Transport aircraft are normally equipped with an anti-skid system. Such a system provides a means of detecting an incipient skid condition of the aircraft tyres and functions to control the brakes to maximise braking efficiency and avoid lock-up of the wheels. Early anti-skid systems were based on the on-off control concept. These were designed primarily to prevent wheel locking and risk of tyre damage. After the introduction of *on-off* type anti-skid systems, it became apparent that braking effectiveness could be increased if the number of anti-skid cycles and their intensity could be minimised. A number of devices utilising various principles of operation have been used for this purpose. These devices predominately utilise the principle of "modulating" brake pressure to keep its value as near as possible to that which will produce a skid. The first generation of modulating systems, released the brake pressure when the computed wheel deceleration exceeded a rate threshold value indicating an incipient skid (known as *quasi-modulating* systems). Currently most transport aircraft have *fully modulating* anti-skid systems which differ from the quasi-modulating systems in the skid control logic. During a skid, corrective action is based on the sensed wheel speed signal, rather than a pre-programmed response.

The braking efficiency that can be achieved depends on the design characteristics of the anti-skid. This is illustrated by Figure 3 which gives an example of the anti-skid efficiency of the three different anti-skid designs as function the maximum friction coefficient of the surface-tyre combination. The efficiency is defined here as the ratio of the average achieved friction over the maximum available friction.

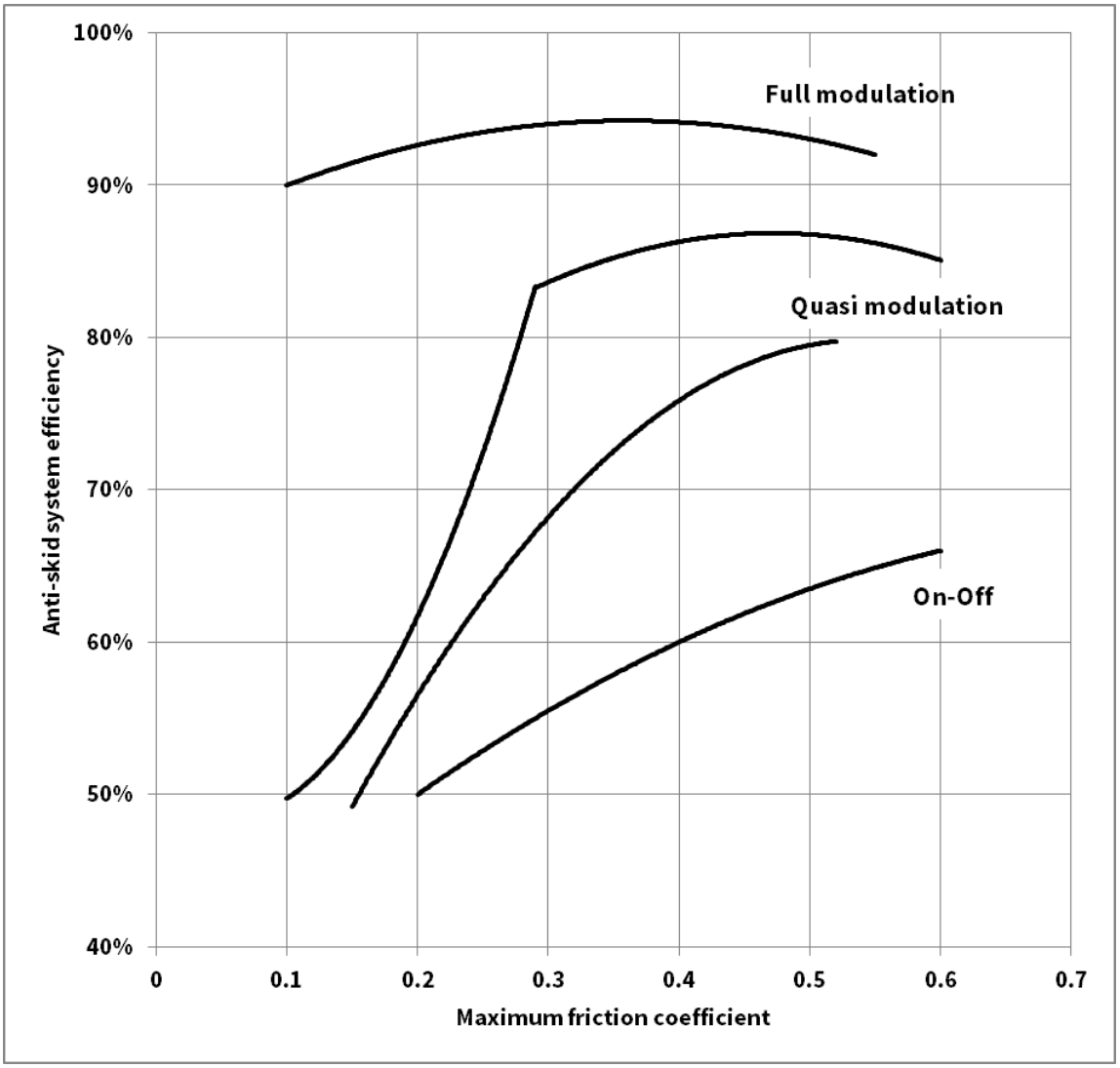

Figure 3: Typical efficiency of different aircraft anti-skid systems as function of maximum friction coefficient[1].

On-off anti-skid systems have the lowest efficiency in obtaining the highest braking friction. Under low friction conditions the efficiency of these systems is further reduced by the low rate at which a wheel regains speed after the pressure has been released. The efficiency of quasi-modulating systems is much better than on-off systems. However the fixed rate threshold used on quasi-modulating does not work well on slippery surfaces as the rate threshold is based on dry runway deceleration. On a slippery runway this means that the braked wheel is entered a skid fairly deeply before action is taken by the antiskid system which reduces the efficiency of the anti-skid system. Fully modulated anti-skid systems have the highest efficiency and are capable of exceeding 90% efficiency even on slippery runways (like flooded runways). Fully modulating systems show much smaller variations in brake pressure around the maximum value of friction. As a result, the average wheel speed remains much closer to the synchronous wheel speed, resulting in a high efficiency. Note that by regulation, the highest efficiency that can be claimed for a fully modulating antiskid system is 92%[4]. Higher efficiency values have been found during flight testing.

IV. Background on the flight testing activities

The research aircraft of NLR, a Cessna Citation II, was used for the flight test programme described in this paper (see Figure 4). Originally designed for executive travel, the Cessna Citation II aircraft (registration PH-LAB) has been extensively modified by NLR to serve as a versatile research and test platform. The aircraft has two Pratt & Whitney JT15D-4 turbofan engines each rated 2,500 pounds of thrust. The aircraft is equipped with a fully modulating anti-skid braking system. The system detects incipient skids by using a wheel speed transducer to measure the deceleration of each landing wheel, and then prevents skids by reducing the brake pressure in proportion to the deviation of each wheel from normal braking deceleration. The system modulates brake pressure to maximize braking efficiency. The left and right wheel brakes are hydraulically operated by independent master cylinders attached to the pilot's and co-pilot's rudder pedals. The brake system is pressurised when either pilot depresses the toe pedals. Interconnect assemblies allow either pilot to operate the brakes with equal authority. The single-wheel main gear used 22 × 8, 24 P.R., type VII aircraft tyres. The tyre inflation pressures were 115 psi for the main-gear tyres and maintained within ±5 psi throughout the course of the test programme. The main gear tyres as well as the brake units were not new. The left hand tyre had a tread depth of 5.2 mm at the start of the test programme and the right hand main gear tyre had a tread depth of 4.8 mm. When the tests were finished this had reduced to 5.1 and 4.6 mm respectively. The aircraft was configured for the Future Sky Safety Contaminated Runway campaign to enable measurement of lateral and longitudinal acceleration, wheel speed rotation by using the aircrafts anti-skid system and pressure in the low pressure pilot brake system. The aircraft was operated by NLR flight crews.

Figure 4: NLR Cessna Citation test aircraft.

The flight testing was executed in the Netherlands at the airport of Twente (EHTW). This airport has a long and wide runway ideally for flight testing. The runway has a Possehl Antiskid top layer with an average macrotexture depth of 1.4 mm. The airport was closed for all other aircraft during the flight tests.

Weather conditions were recorded by an official weather station next to the runway. Also some weather data like temperature and static pressure were recorded on-board of the aircraft. The tests were conducted over two consecutive days. During the first day of testing the air temperature varied between 27 and 29 deg. C. Wind speeds varied between 7-10 kt. with a mean direction of 67 deg. There were no clouds during the first day of testing. During the second day the weather had changed. The air temperature now varied between 19 and 21 deg. C. The wind speed varied between 8-11 kt. with a mean direction of 190 deg. During the second day the sky was mainly clouded. However, no precipitation was recorded.

The objective of the test programme required a runway covered with a target depth of 15 mm of standing water. The build-in cross slope of a runway prevents that such a quantity of water stays on the runway, unless there is heavy rainfall. A water pond is therefore needed to create an area of sufficient water depth that stays at this level for long enough time for an aircraft to pass. Such water ponds are normally constructed using flexible re-enforced rubber strips as dikes to contain the water. These rubber strips are then put into grooves that are cut into the runway surface (see Figure 5). This is a classical way of building a water pond on a runway. It has been used for water certification ingestion tests as well as for braked tests with a wide range of civil transport aircraft since the 1960s.

Figure 5: Flexible rubber strip in a runway groove.

The runway at Twente did not have a water pond facility at the start of the project. This facility had to be constructed. A classical water pond consists of series of grooves into which flexible rubber strips are put to form dikes. To gain some experience with such a setup, a small test pond was constructed at the NLR premises before making one at Twente airport. This water pond measured 4 by 10 m and is shown in Figure 6 (empty). The test pond was filled to several water levels. Experiences were gained in grooving, fixing the rubber strips into the grooves, measuring of water depths and managing leakage of the pond.

Figure 6: Test water pond.

After positive experiences gained with the test water pond it was decided to construct a water pond at the flight test location. The runway at Twente airport has a very consistent longitudinal slope of 0.2% along the runway. Likewise the cross slope is also very consistent along the runway being 0.6-0.8% at the runway centreline and 1.5-1.6% further away from the centreline. The longitudinal slope required that several rubber cross dams had to be constructed to get reasonable consistent water levels in the water pond. These cross dams were placed every 7.7 m to form 13 separate sections. The final water pond on the test runway is shown in Figure 7. As the aim of the flight tests is to analyse braking performance it was not necessary to have the nosewheel running through the water. Therefore no pond was construction for the nosewheel to run through. Keeping the centre part dry also provides additional controllability in case the aircraft deviates from its track during the test run.

Figure 7: Water pond at Twente airport.

The overall length of the water pond was 100 m. This is sufficient long to obtain useful test data. Braked tests done by NASA used a water pond of similar length. The water pond starts 1.15 m from the centreline and stretches to 5 m from the centreline. The target average water depth in the water pond at the main wheels was set to 15 mm. Along each section the actual water depth will normally vary both in longitudinal as well as in lateral direction as the test section is not completely flat. However the main gear tyres should be exposed to target water depth when the

aircraft does not deviate significantly from the runway centreline. Deviations from the centreline were observed on a few test runs, however, these were not significant enough to influence the test results.

The water pond was filled to the target depth using water trucks as shown in Figure 8. Water depths were measured using a specially constructed wedge which is shown in Figure 9. Prior to each run water depth measurements were taken and recorded at pre-defined positions in each section of the water pond (see Figure 10). These positions matched the location of the main gear tyres. If the water depth was well off the target value, water was either removed from the section or added. High winds can make it difficult to maintain consistent water levels. Based on previous experiences with water pond testing a maximum wind speed of 12 kt. was defined for the test programme. Figure 11 and Figure 12 show the surface of the water pond under calm and light windy conditions. In order to minimise the influence of wind on the water depth measurements, a metal ring was placed around the water depth gauge as illustrated in Figure 13.

Figure 8: Filling of the water pond.

Figure 9: water depth gauge.

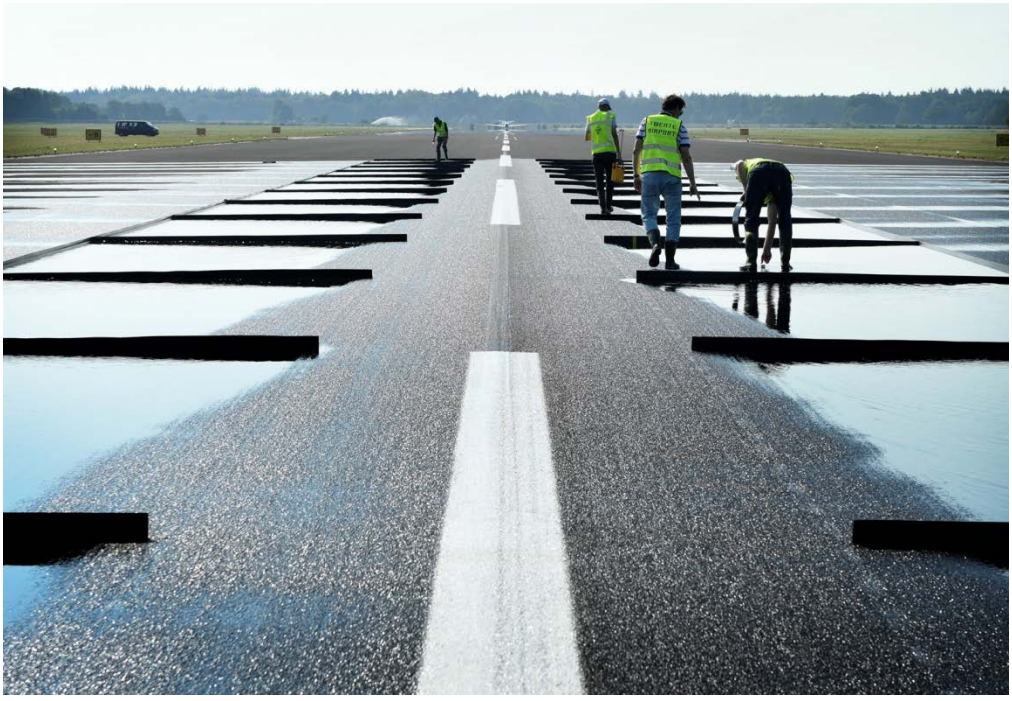
Figure 10: Example of measuring water depth level in each section.

Figure 11: Water pond in calm wind conditions.

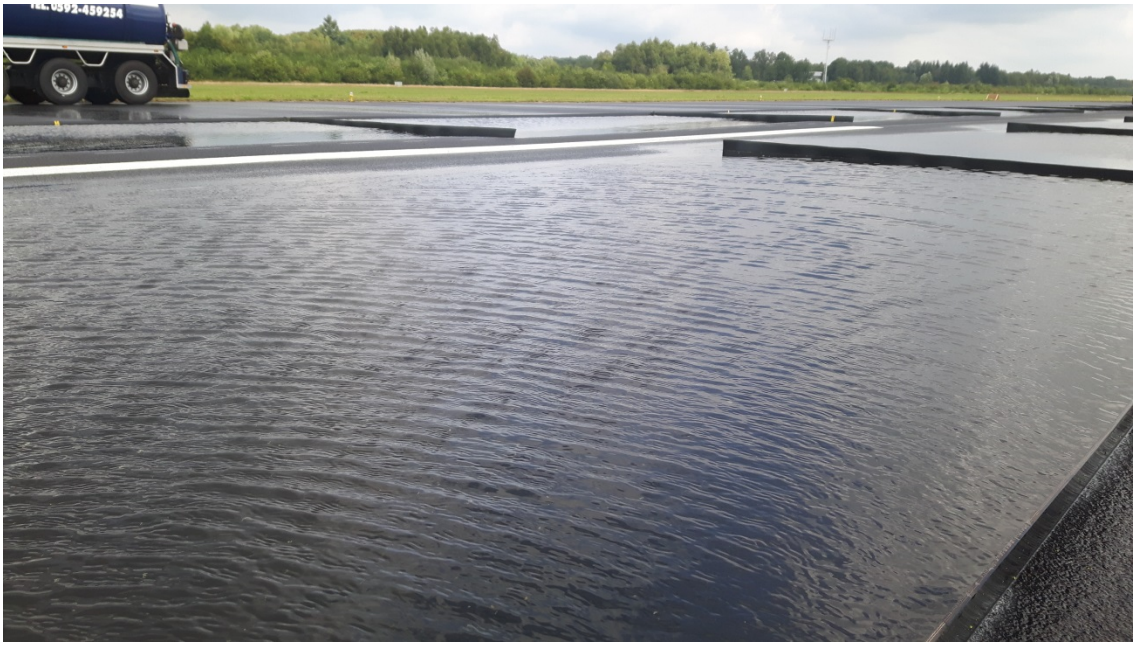

Figure 12: Water pond at 8 kt. wind.

Figure 13: Measuring of water depth using a metal ring around the water depth gauge.

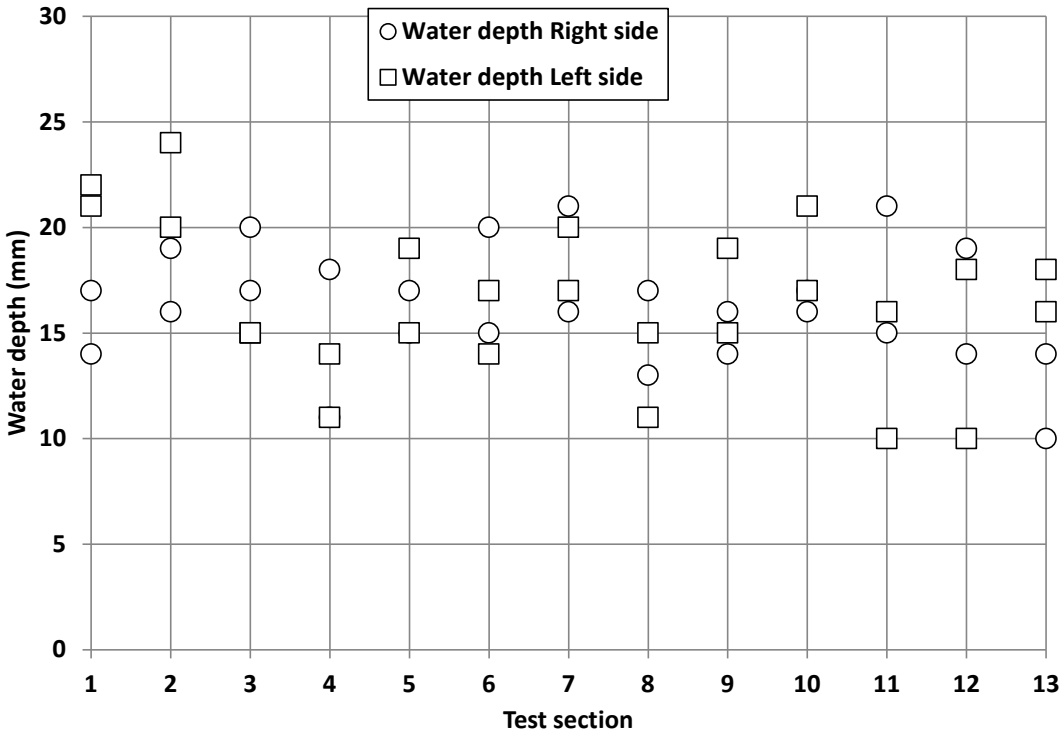

Figure 14: Example of the water depth levels measured along the water pond (numbers refer to section).

The target water depth was set to 15 mm at the main gear tyre track. This is slightly above the normal certification limit of 13 mm for transport aircraft. In many of the earlier flight tests on flooded runways the water depth was much less and close to the wet-flooded runway threshold of 3 mm as defined in the regulations (see e.g. Ref. 4). For the present tests a high water depth was chosen as this is more representative to a runway under extreme rain conditions. During the test programme the overall average water depth level was somewhat higher than this target (16.7 mm). This was not considered a major issue for the objectives of the project. An example of the measured water depths in the different test sections is shown in Figure 14. Two measurements were taken in each left and right section. The direction of flight is from section 1 to 13.

The test matrix was developed keeping in mind how the data reduction process would be done. As an aircraft passes through the water pond, the tyres displace the water. This causes a drag force acting on the tyres called displacement drag. Water thrown up by the tyres could hit the airframe causing an impingement drag force (see Figure 15). To account for these drag forces tests runs in an unbraked condition were required. Therefore the test matrix had to incorporate both an unbraked and a braked run for a given target entry speed. It is important that true airspeed and ground speed during the water pond passage are more or less equal for both test pairs. The aircraft weight should be similar or equal in both test-pairs, as well as the average water depth and control surfaces deflections. The aircraft was tested with flaps in the up position during all runs to minimise potential damage to the flaps and to obtain the highest test speeds in the water pond. The maximum test speeds are determined by the rotation speed of the aircraft which depends on flap setting and aircraft weight. A flaps up setting ensures the highest achievable speeds for the chosen flight test approach. Table 1 shows the test matrix. The runs were arranged in such a way that there was a build-up approach as to the water pond entry speeds which increased 10 Kt. between each two runs. This was done from a flight safety point of view. Some high tests runs were repeated to validate the results.

Initially is was felt that at higher speeds test runs with half the braking input would be needed to make the test pilots aware of the aircraft behaviour. However, during the actually testing it was decided that these partial-braked runs were not needed (test points 6, 9 and 12).

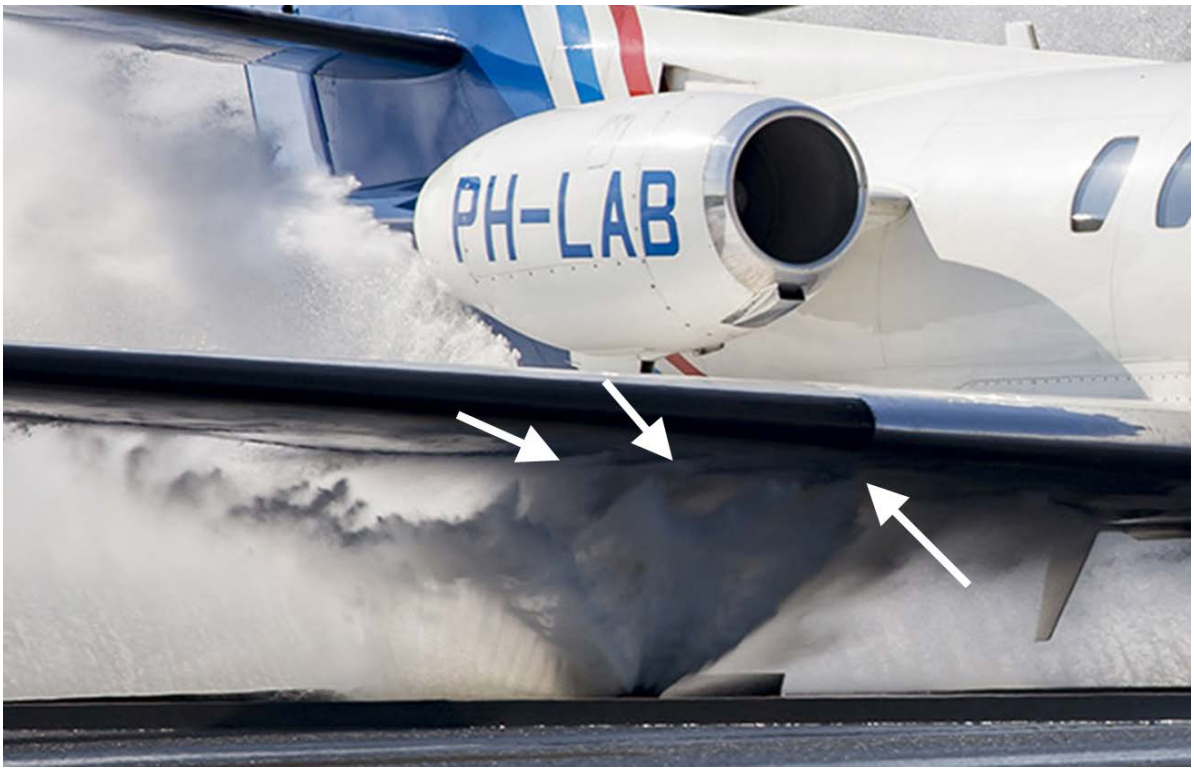

Figure 15: Water spray hitting the airframe.

Table 1: Test matrix

Test number	Flight Configuration (Weight and Flaps)	Engine setting	Target water pond entry speed IAS (kt.)	Description
1	Takeoff, takeoff weight, flaps configuration up	Idle	60	Unbraked
2	Takeoff, takeoff weight, flaps configuration up	Idle	60	Maximum braking
3	Takeoff, takeoff weight, flaps configuration up	Idle	70	Unbraked
4	Takeoff, takeoff weight, flaps configuration up	Idle	70	Maximum braking
5	Takeoff, takeoff weight, flaps configuration up	Idle	80	Unbraked
6	Takeoff, takeoff weight, flaps configuration up	Idle	80	half pressure/moderate braked
7	Takeoff, takeoff weight, flaps configuration up	Idle	80	Maximum braking
8	Takeoff, takeoff weight, flaps configuration up	Idle	90	Unbraked
9	Takeoff, takeoff weight, flaps configuration up	Idle	90	half pressure/moderate braked
10	Takeoff, takeoff weight, flaps configuration up	Idle	90	Maximum braking
11	Takeoff, takeoff weight, flaps configuration up	Idle	100	Unbraked
12	Takeoff, takeoff weight, flaps configuration up	Idle	100	half pressure/moderate braked
13	Takeoff, takeoff weight, flaps configuration up	Idle	100	Maximum braking

For each test run the water pond was filled to the target water depth level. The aircraft was positioned at a pre-determined distance from the water pond. As soon as the water pond was ready, a static takeoff was commenced. The engines were set to idle at a marked position before the water pond. The position of the idle thrust marker and the position for the static takeoff were determined as such as the aircraft would enter the water pond near the target speed and with the engines in idle thrust. The calculations for this were done using an in-house developed performance program. The results of these calculations were validated before conducting the actual tests with the water pond. An example of a typical run is shown in Figure 16. This shows the time-history plot of the (uncorrected) longitudinal acceleration and the ground speed. As can be seen from the plot the aircraft is accelerated to a certain speed from the static takeoff point. After reaching the idle marker the engines were set to idle at which the normal acceleration starts to drop. As the aircraft reaches the water pond the aircraft is slightly decelerating due to aerodynamic and rolling friction forces being larger than the idle forward thrust. This was the case for all test runs conducted. When entering the water pond the aircraft starts to decelerate more as illustrated in Figure 16. Depending on the test point the test pilot would apply maximum brakes or leave the aircraft rolling without brakes being applied. During a braked test run, maximum brakes were applied by the pilots just when the aircraft had entered the

water pond (see Figure 17). Just before leaving the water pond the brakes would be released again (see Figure 17). Between each run sufficient time was taken for the brakes to cool down. Also the airframe and tyres were inspected for damages after each run. Video recordings and still images were made from the outside and inside the aircraft. These images were used in case water ingestion into the engines was suspected (see e.g. Figure 18). The videos and still images were also used in the post processing to analyse spray patterns for hydroplaning indications.

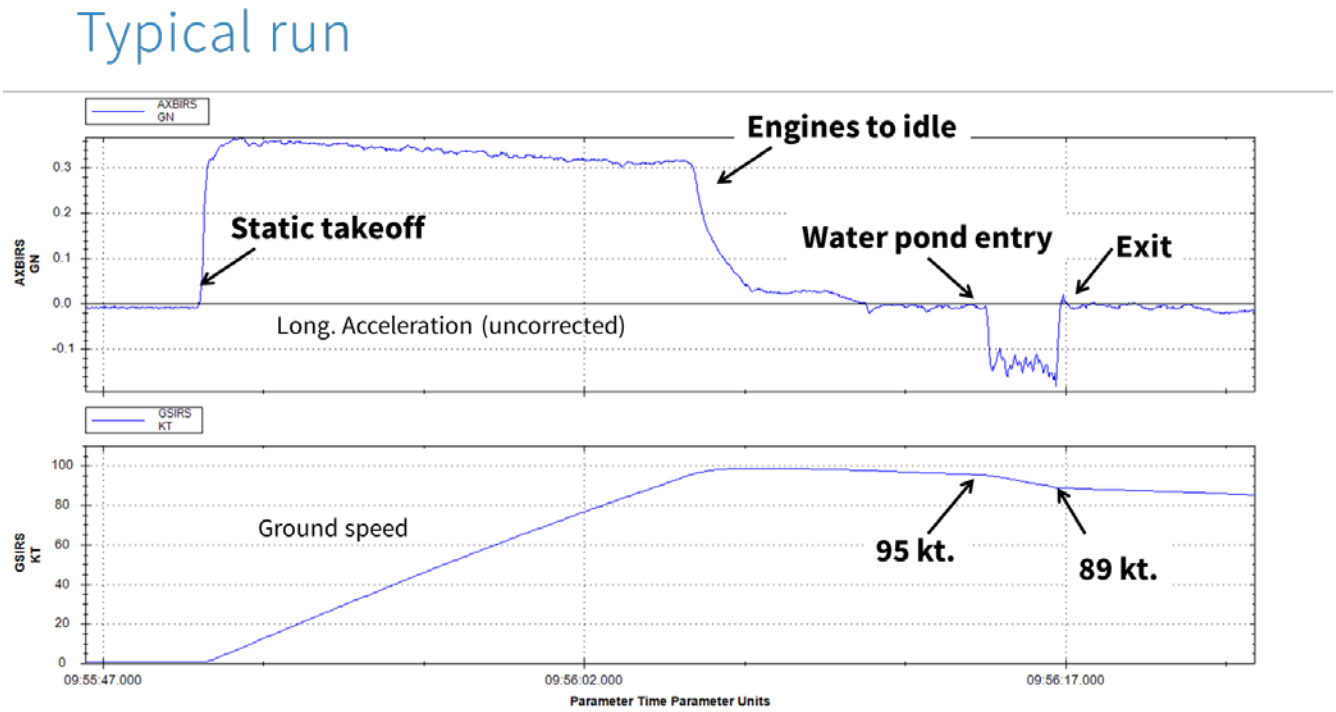

Figure 16: Longitudinal acceleration and ground speed time-history plot for a typical test run.

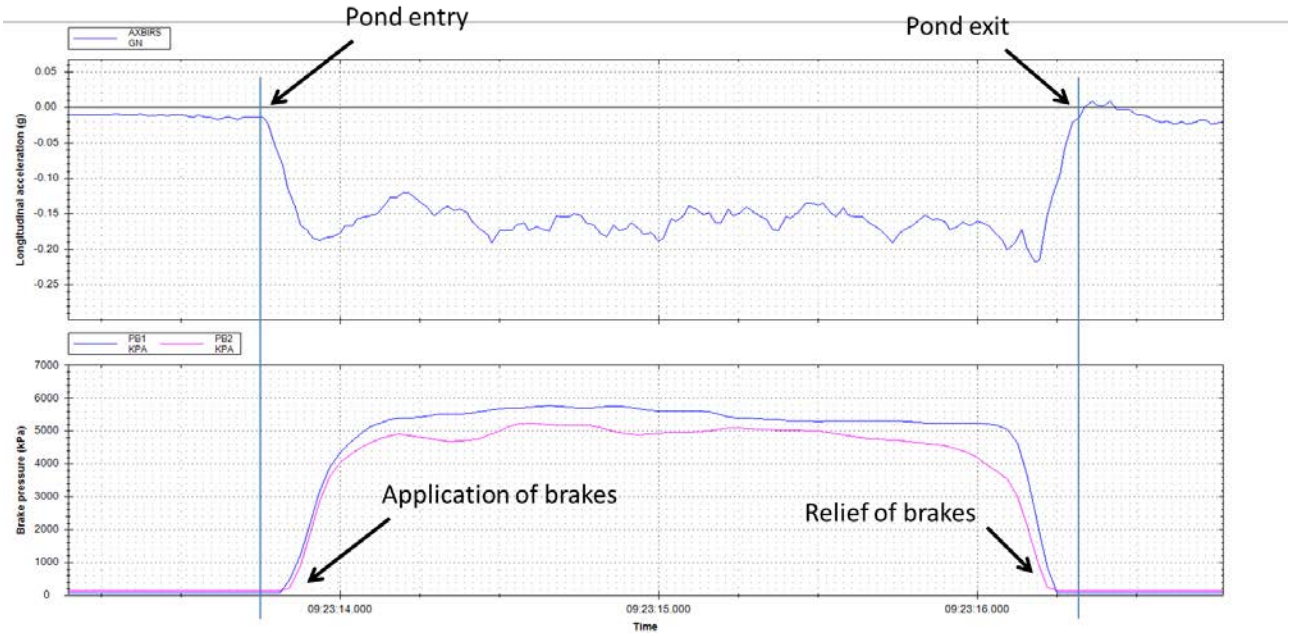

Figure 17: Example time-history plot of longitudinal acceleration and brake pressure when running through the water pond (ground speed between 85-78 Kt.).

Figure 18: Cessna Citation test aircraft running through the water pond.

V. Data reduction and analysis

Different parameters were recorded on board the test aircraft, including acceleration, airspeed, ground speed, engine parameters, brake pressures, and wheel speeds (see Table 2 for complete list) at (high) sample rates along with appropriate environmental measurements such as temperature, pressure, wind speed and direction. Weather data were taken from an official weather station that is located next to the runway. Weight and centre of gravity were determined before each test run. Water depth in the water pond was measured prior to each test run at 26 fixed locations. These locations were marked in the pond and corresponded to the lateral position of the main gear tyres. Uniformity in pilot brake application and proper aircraft configuration for a given series of test runs was determined from review of the time-history plots. The measured longitudinal acceleration was corrected for biases and pitch angle influence. The acceleration data were also smoothed using a special moving average algorithm.

The objective of this project is to establish the effective braking friction coefficient on a flooded runway as function of ground speed. The effective braking friction coefficient is defined by:

$$\mu_{EFF} = \frac{F_{Brake\_main}}{N_{main}}$$

This equation requires the braking force exerted on the main wheels and the normal load on the main wheels. As already noted, there are several forces acting on the aircraft when running through the water pond. From the aircraft performance database, information on aerodynamic drag, rolling friction and idle thrust can be obtained. However, the water layer also causes additional drag forces: tyre displacement drag and water impingement drag. From a braked run through the water pond it is not possible to differentiate between these last two forces and the main gear braking force. Therefore an unbraked run at nearly the same speed, weight and water depth as done for the braked run was conducted. By subtracting the measured deceleration force of the unbraked test run from the measured deceleration force in the braked run, the braking friction force is obtained.

With the recorded on board data, the normal load N_{main} acting on the main gear tyres can be derived for the test aircraft taking into account the force-moment diagram of the aircraft. For the derivation of the normal load, data on

aerodynamics and engine thrust are also needed. Idle thrust data were obtained from the engine deck. Aerodynamic drag and lift data were obtained from Cessna. Data on pitching moments were estimated using available aerodynamic data for a Cessna Citation 500.

VI. Flight test results

A. Introduction

In this section the main results obtained from the flight tests data are presented. An example of data recorded is shown in Figure 19. This shows a number of recorded parameters from a few seconds before entering the water pond and after leaving the pond. The example also shows the corrected longitudinal acceleration as well as the longitudinal acceleration derived from the ground speed. As the ground speed was sampled at a high rate, differentiation of this speed leads to reasonable accurate normal acceleration data in the direction of travel (without having to correct it for pitch angle). This ground speed derived acceleration was used to cross check the directly measured (and corrected) longitudinal acceleration used for the analysis. During flight testing it was discovered that the wheel speed of the right main gear wheel was not recorded correctly in most of the runs. This anomaly could not be fixed during the test programme. Only wheel speeds of the left main gear tyre could therefore be used for analysis.

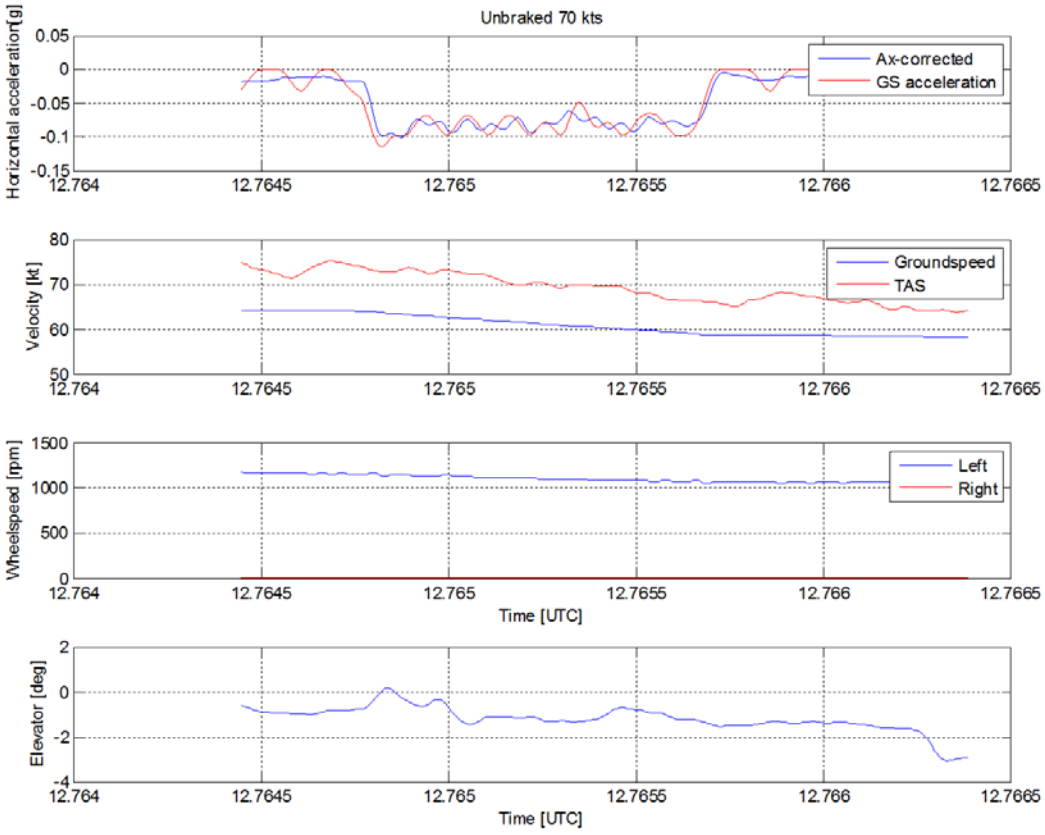

Figure 19: Example of time-history plots.

Table 2: Overview of parameters recorded on board as function of time.

Parameter	Sample rate
Normal acceleration, Lateral acceleration, and Longitudinal acceleration	50 Hz
Groundspeed	10-20 Hz
True airspeed	8 Hz
Airspeed	8Hz
Pilot commanded brake pressures	20 Hz
Pitch angle	50 Hz
Heading	50 Hz
Left and right engine N1	20 Hz
Left and right engine N2	20 Hz
Elevator position	64 Hz
Rudder	64 Hz
Aileron	64 Hz
Angle of attack	50 Hz
Main wheel speeds	50 Hz
Static temperature	2 Hz
Static pressure	2 Hz
Flap position	20 Hz
Speed brake position	20 Hz
Fuel mass flow Left engine	20 Hz
Fuel mass flow Right engine	20 Hz

B. Measured effective braking friction

The effective braking friction coefficients derived from the test data are shown in Figure 20 as function of ground speed. As clearly illustrated the braking friction coefficient rapidly reduced as ground speed increases. Above 80 Kt. only very low friction levels are found, similar to an icy runway. As part of a different project, the Cessna Citation was also tested on the same runway under wet conditions. The runway was artificially wetted for these tests and the water depths varied between 0.4-1.3 mm. Runways with a water depth up to 3 mm are considered to be wet. Figure 21 shows a comparison between the wet and flooded runway braking capabilities of the Cessna Citation II test aircraft. The impact of the flooded runway on the braking capabilities is significant. The dry runway effective braking friction coefficient of the Cessna Citation II test aircraft was determined from separate tests to be around 0.48 for ground speeds below 120 kt.

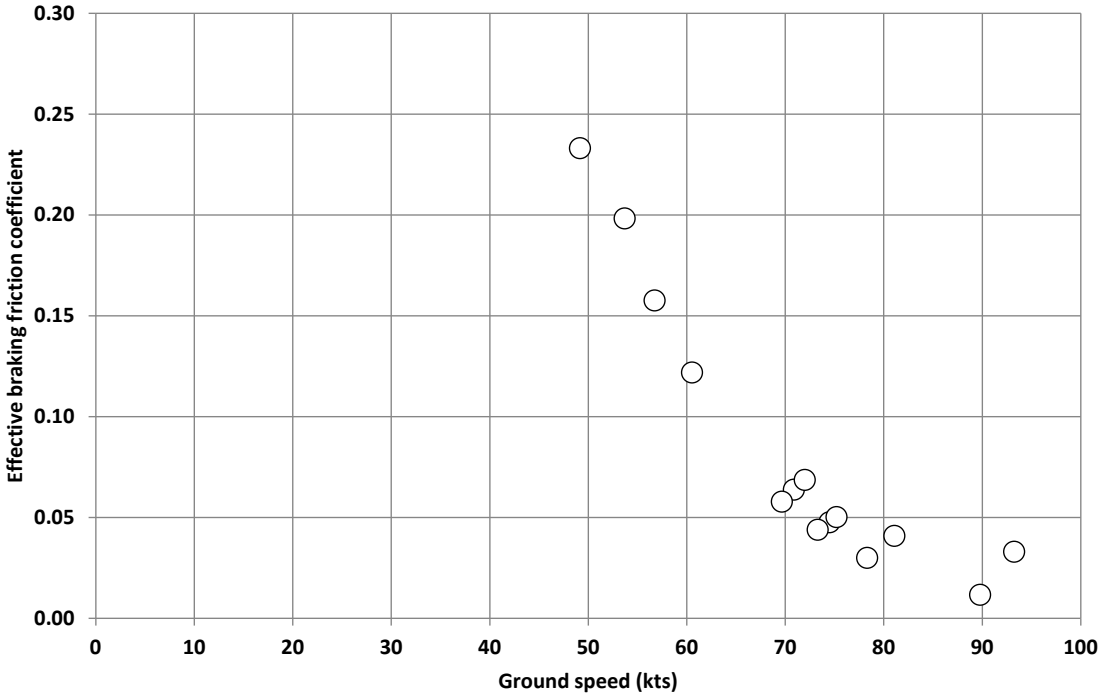

Figure 20: Effective braking friction coefficient as function of ground speed for the Cessna Citation II on a flooded runway.

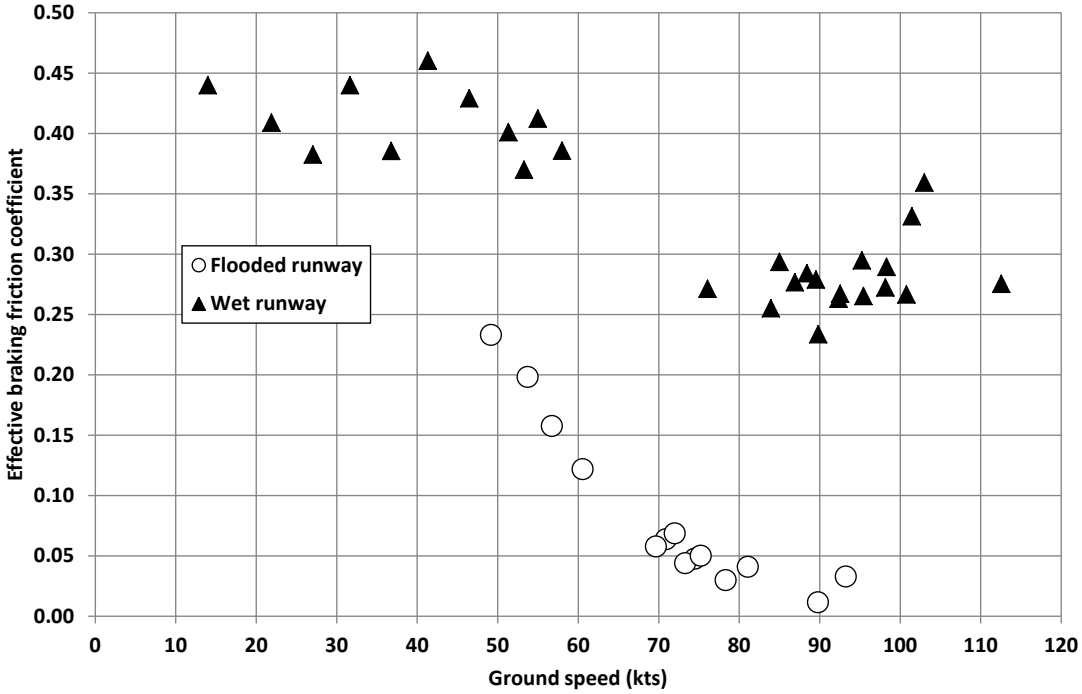

Figure 21: Comparison of wet and flooded runway braking capabilities of a Cessna Citation II.

C. Water contamination drag

From the unbraked tests it is possible to derive the contamination drag due to the water displacement by the main gear tyres and impingement drag caused by the water spray generated by the main gear tyres. For this derivation the longitudinal acceleration just before the water pond entry and after exiting the water pond is subtracted from the longitudinal acceleration measured in the water pond. This acceleration is then multiplied with the aircraft mass to obtain the contamination drag. The derived contamination drag is compared to results obtained in an previous test programme (although at a lower water depth) and to a theoretical model provided by e.g. EASA AMC 25.1591[4]. This model is presented here for completeness.

A tyre running through a layer of water experiences additional drag due to the displacement of the fluid. This displacement drag is modelled using the analogy with aerodynamic drag and for a *single tyre* is given by[4]:

$$\mathbf{D_d = \frac{1}{2}\rho V_g^2 S C_{Ds} f_H}$$

The reference area S in this equation is defined as: $S = d\, b_s$ with d being the water depth and b_s the tyre width at fluid surface given as[4]:

$$\mathbf{b_s = 2W\left[\frac{\delta + d}{W} - \left(\frac{\delta + d}{W}\right)^2\right]^{0.5} \quad for \left(\frac{\delta + d}{W}\right) \leq 0.5}$$

The tyre vertical deflection δ is a function of the normal load on the tyre and tyre inflation pressure amongst others.

For most aircraft tyres the drag coefficient C_{Ds} varies between 0.70 and 0.80. An average of 0.75 is normally used and recommended for aircraft performance calulcations[4]. When the ground speed reaches the hydroplaning speed the displacement drag reduces. At this speed the tyre is separated from the runway by a water film. As the tyre is planning over a water film, less water is displaced and as a result the displacement drag reduces as speed increases beyond the hydroplaning speed. Different empirical formulae have been developed to account for this effect. Most of these formulae give very similar results. EASA AMC 25.1591 provides a graph showing the hydroplaning decay correction f_H (Ref. 4).

Figure 22 gives a comparison of the contamination drag for the main wheels derived in the present test programme to earlier tests conducted by NLR and EASA AMC 25.1591 model results. Note that the test aircraft in these previous tests had a slightly higher main gear tyre inflation pressure then in the present tests. As shown in Figure 22 the predicted water contamination drag is somewhat lower than measured. This is caused by the impingement drag which is not accounted for in the model. In particular the bow wave causes additional drag from the forward spray hitting the airframe (mainly the wing in case of the Cessna Citation test aircraft, see Figure 23). In front of the tyres a bow shaped wave front can develop at speeds greater than the surface wave as water builds up ahead of the tyre, ejecting a spray in forward and upward direction. The drag on the airframe by the forward spray depends upon where in the trajectory of the forward spray the aircraft catches up with the spray. If this occurs near the maximum height point of the trajectory then there would be a high impingement drag. However if this point is near the maximum forward point of the trajectory, hardly any impingement drag from the forward spray will be noticed. In case of the Citation test aircraft it is somewhere in between both of these extremes. Finally also some water sprayed backwards hit the wing and fuselage of the test aircraft causing additional impingement drag.

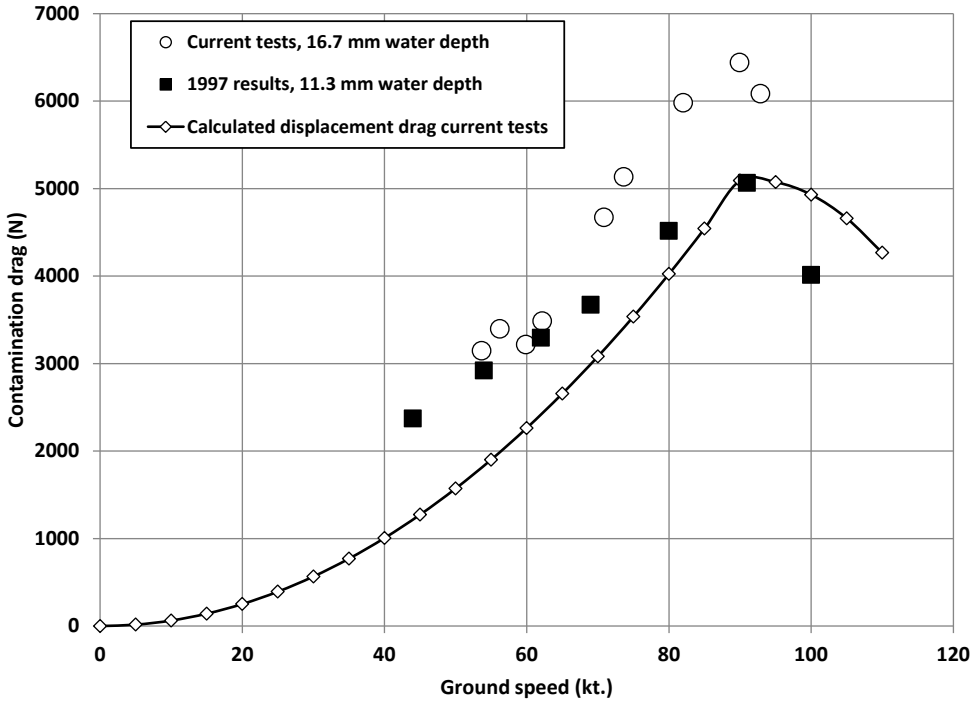

Figure 22: Comparison of contamination drag derived in the present test programme to earlier tests and predictions.

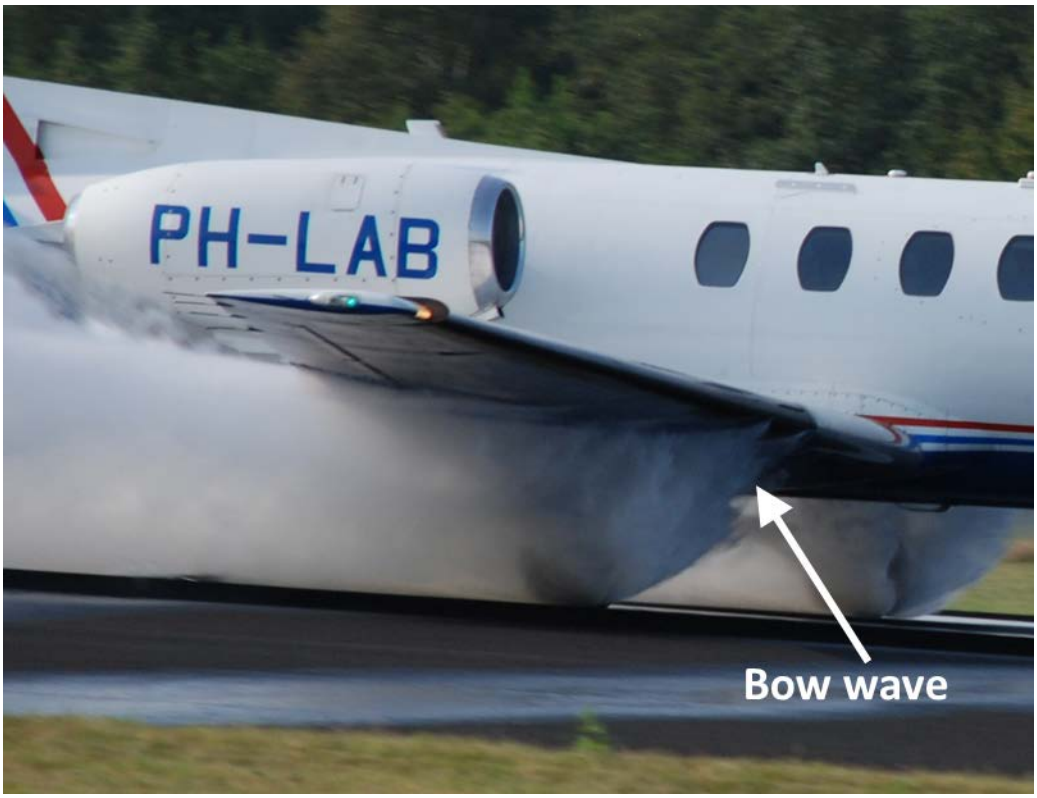

Figure 23: Bow wave hitting the wing.

D. Derived hydroplaning speeds

Hydroplaning is defined as the condition under which the tyre footprint is lifted off from the water covered runway surface by the action of the fluid. The forces from the fluid pressures balance the vertical loading on the wheel. Considering the high water depths used in the present flight tests, dynamic hydroplaning will have a significant influence on the braking performance. The test runway surface has a harsh microtexture which limits the influence of viscous hydroplaning. The onset of full dynamic hydroplaning is not easy to determine. There are several manifestations of dynamic hydroplaning that can be observed from flight tests: tyre bow wave suppression; fluid drag peaks; and, tyre spin-down. These manifestations can be used to determine the dynamic hydroplaning speed of a tyre. Earlier experiments have shown progressive reduction of the bow wave spray angle as ground speed increases. Above the full (dynamic) hydroplaning speed the bow wave disappears completely. This information can be obtained from still photo images and videos recordings which were taken during the water pond tests. As the tyre reaches and exceeds the full hydroplaning speed, displacement and impingement drag start to reduce. The strongest indication of a full (dynamic) hydroplaning is the condition of unbraked wheels slowing down or stopping completely. The fluid dynamic lift force under the tyre causes the centre of pressure of vertical ground reaction to move ahead of the wheel axle with increasing ground speed. This causes a spin-down moment. At the hydroplaning speed this spin-down moment will exceed the total spin-up moment caused by all tyre drag forces. The tyre will start to spin-down and can come to a complete stop. Above the hydroplaning speed the centre of pressure of vertical ground reaction moves back to the wheel axle. As this time the tyre will start to spin-up again. As a general rule of thumb the wheel speed should be less than 50% of that on a dry runway to have total dynamic hydroplaning. To analyse this wheel speed of the tyres need to be recorded during the flight tests. The wheel speed of the main gear tyres need to be related to the wheel speed obtained on a dry runway at the same ground speed. This relation can be obtained from the recorded wheel speeds prior to entering the water pond and just after exiting the water pond. The still images taken during the test runs indicate that the bow wave is suppressed at higher ground speeds starting from 84 Kt. as shown in Figure 24. The bow wave is more or less flat at a speed of 92 Kt. This would suggest that the full hydroplaning speed is somewhere between 84 and 92 Kt. The contamination drag plot as function of ground speed (shown in Figure 22) suggests a peak in the drag at around 90 Kt. This plot only has a very few number of data points around this peak so this is not conclusive regarding the hydroplaning speed. Finally the wheel speed of the left main gear wheel is analysed. As noted the recording on the right main gear wheel were not useable. The minimum ratio between wheels speed in the water pond and the expected wheel speed on a dry surface as function of ground speed is shown in Figure 25. This plot shows that the wheel speed has drop below 50% of that on a dry runway at 92 Kt. ground speed (see also Figure 26). This would mean that full hydroplaning occurred below 92 Kt. but above 84 Kt. Although the number of data points is limited, Figure 25 suggests a hydroplaning speed of around 90 Kt. Based on the above discussed data, the full (dynamic) hydroplaning speed is estimated to be 90 Kt. (ground speed). This also corresponds to the very low braking friction values shown in Figure 20 at and above this speed. It must be noted that determining hydroplaning speeds from flight test data is not an exact science even if all indicators for hydroplaning are available. It is only a best estimate of the dynamic hydroplaning speed. The dynamic hydroplaning speed of 90 Kt. corresponds to $8.4\sqrt{p}$, which matches with the trend for modern cross-ply tyres shown in Figure 2.

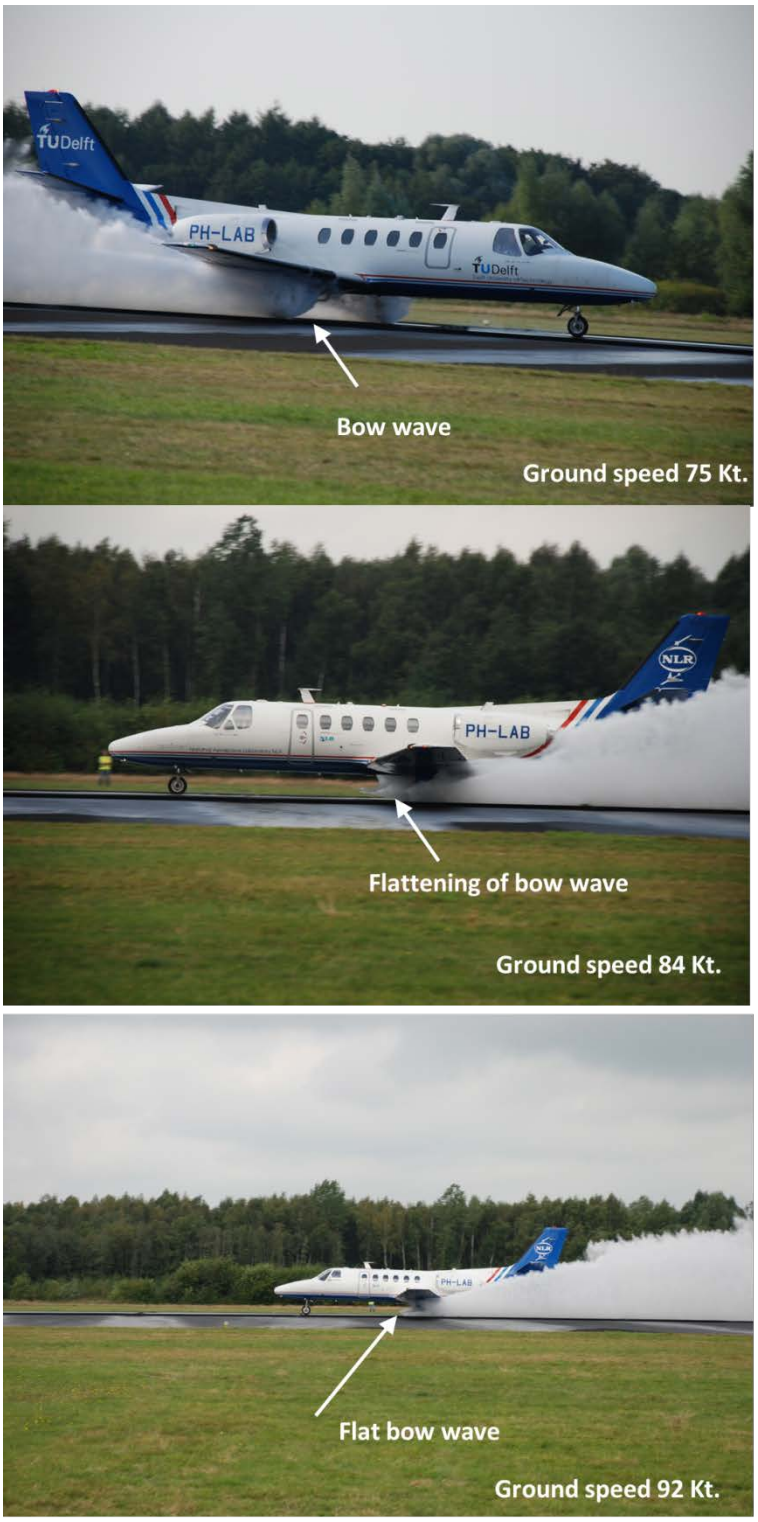

Figure 24: Bow wave development.

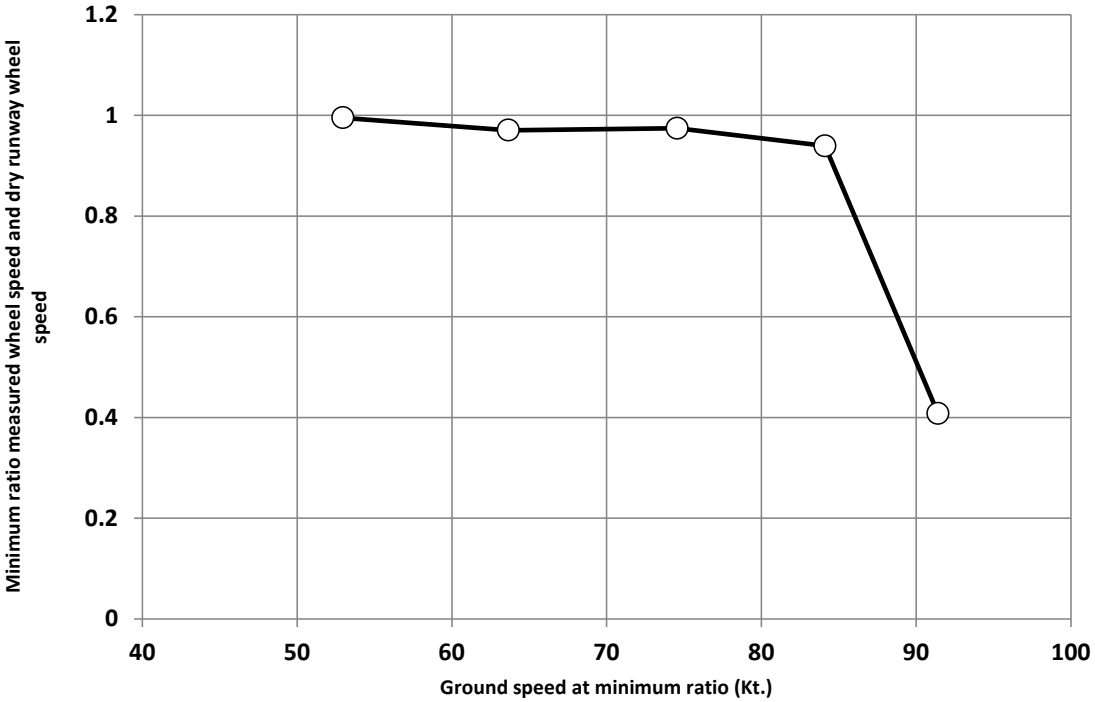

Figure 25: Minimum ratio between wheels speed in water pond and expected wheels speed on a dry surface as function of ground speed.

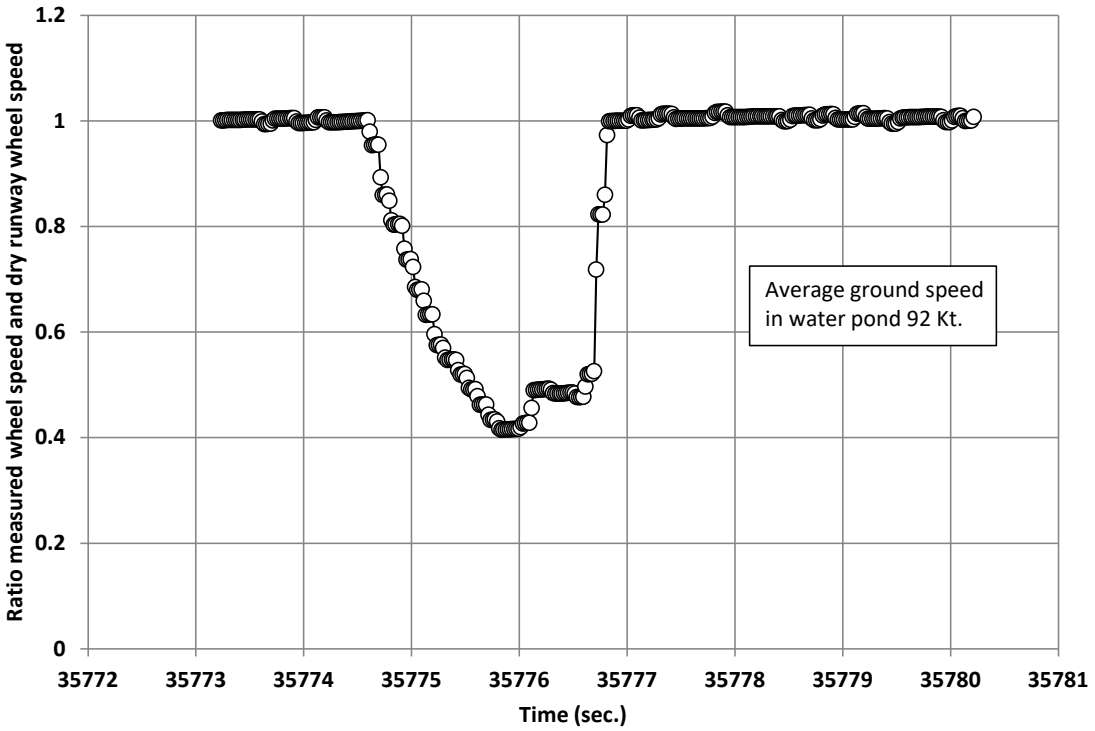

Figure 26: Relative wheel speed left main gear tyre.

Braked runs cannot be used to estimate the hydroplaning speed of the Citation test aircraft as discussed next. However, they can provide insight in how the brake system functions in particular the anti-skid system. The anti-skid system is only active if the pilot meters a pressure in excess of that required to skid the tyre. The system then immediately reduces the braking level to minimise the depth and duration of the skid. This allows the wheel to spin back up, generating a reference speed for the anti-skid system. The anti-skid then immediately allows braking to re-apply at a lower level. The pressure will be allowed to gradually increase again until either another skid occurs or the pilot's metered pressure is achieved. The anti-skid does not apply pressure on the brakes, but only relieves it. This whole process is conducted at a very high frequency (typically 200 Hz), allowing the anti-skid to react quickly to changes in runway slipperiness. When brakes are applied during severe tyre hydroplaning, the anti-skid system may lose its reference speed as the wheels are not spun up. The wheels remain locked up until the pilot released the brake pedals. On some aircraft this problem is solved by using the groundspeed signals from the aircraft's inertial reference system as a backup wheel reference speed. On aircraft with a bogie main landing gear the rear wheels are used as a reference speed in preventing locked wheels conditions. The Cessna Citation II has a locked wheel crossover protection system installed. This prevents loss of aircraft control caused by unequal wheel rotation rates. When the anti-skid system detects that one main gear wheel is rotating 50% slower than the other, brake pressure to the slow wheel is dumped, allowing wheel speeds to equalise. The 50% tolerance between the wheel speeds is provided to permit an amount of differential braking, for steering purposes. Locked wheel crossover protection is functional at ground speeds greater than 40 knots on the test aircraft. This level of protection is not available if both wheels are locked. The full hydroplaning speed of the main gear tyres was estimated from unbraked runs to be 90 Kt. Just before this ground speed the wheels start to spin-down. If full brakes are then applied lockup of the wheels can occur. The locked wheel crossover protection system cannot prevent this from happening as the system will not detect that one main gear wheel is rotating 50% slower than the other as both are spinning down due to hydroplaning. This is illustrated in the wheel speed data shown in Figure 27 for ground speeds higher than the full hydroplaning speed. Just after entry of the water pond full brakes are applied. Immediately the wheel speeds drops to zero for both left and right main gear wheels. Only after relieving of the brakes the wheels start turning again. At lower ground speeds locked wheel conditions were not recorded. This means that the anti-skid system remained active.

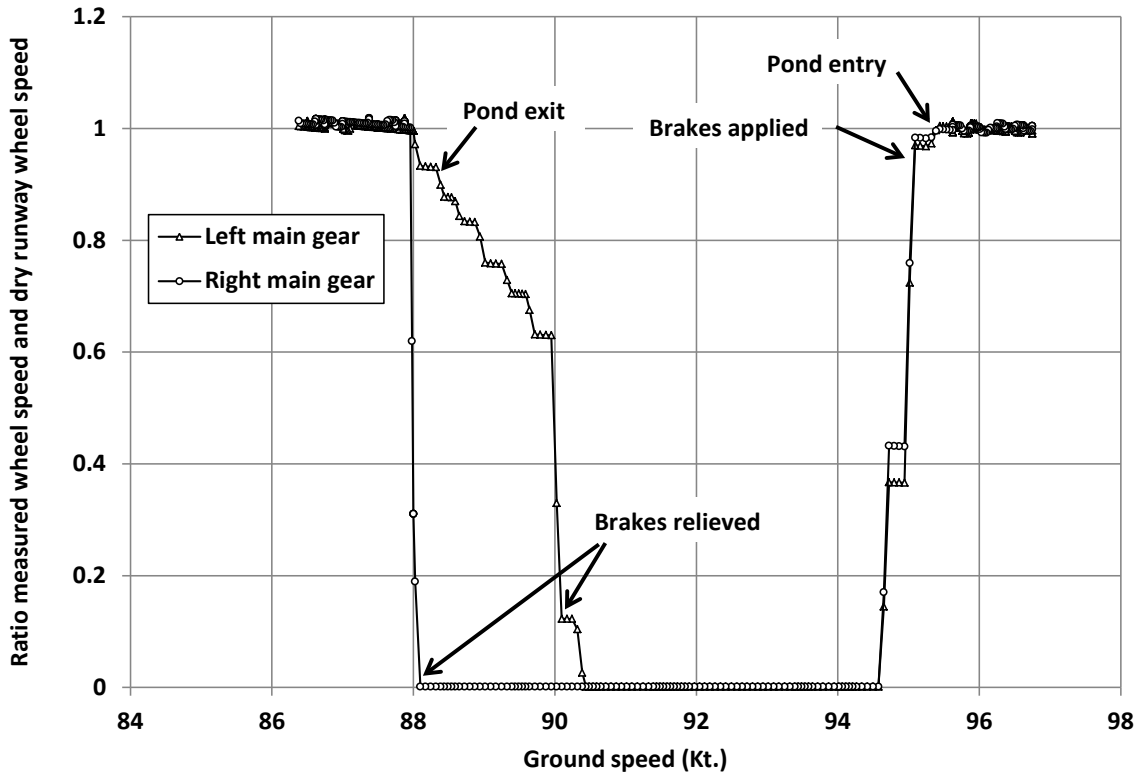

Figure 27: Relative wheel speed as function of ground speed when running through the water pond in a braked condition.

VII. Conclusions

A substantial number of tests with specially instrumented Cessna Citation II aircraft have been conducted on a flooded runway condition. These tests were conducted as part of Project P3 of the Future Sky Safety Programme to obtain a test data and a better understanding of aircraft ground handling performance flooded runway conditions. Major Test Findings are:

- Ground speed was identified as major a factor that influences flooded-runway tyre friction performance;
- The tyre friction performance for flooded runway conditions is significantly less than for a wet runway;
- Hydroplaning has a large influence on the anti-skid performance of the Cessna Citation test aircraft. It is shown that locked wheel conditions can occur despite the locked wheel crossover protection system.

It is recommended to use the test data obtained with the Cessna Citation II aircraft for the evaluation of EASA AMC 25.1591[4] and for analysing models for predicting braking performance of aircraft tyres on flooded runway conditions.

Acknowledgments

This research was funded from the EU's Horizon 2020 Research and Innovation Programme under Grant Agreement No. 640597. This paper does not necessarily reflect the views of the European Commission. The author wishes to thank Thomas J. Yager (Distinguished Research Associate, NASA Langley Research Center), for sharing his experiences on flooded runway braking tests at NASA.

References

[1] Van Es ,G.W.H.," Review of the state of current knowledge regarding tyre braking performance, anti-skid systems, and modern aircraft tyres on water contaminated runways," EU Joint Research Programme (JRP) on Safety, Future Sky Safety deliverable D3.2, 2015.

[2] Horne, W. B. and Upshur, T.J, "Pneumatic Tyre Hydroplaning and Some Effects on Vehicle Performance," Society of Automotive Engineers, SAE paper 650145, 1965.

[3] Van Es, G.W.H.., "Hydroplaning of modern aircraft tyres," National Aerospace Laboratory NLR, NLR-TP-2001-242, 2001.

[4] Anon.," Certification Specifications and Acceptable Means of Compliance for Large Aeroplanes CS-25," European Aviation Safety Agency EASA, Amendment 18, 22 June 2016.